Biophysical Chemistry 13 (1981) 265–273
North-Holland Publishing Company

DIELECTRIC BEHAVIOR OF POLYELECTROLYTES. II. THE CYLINDER

Phyllis I. MEYER, Gary E. WESENBERG and Worth E. VAUGHAN
Department of Chemistry, University of Wisconsin-Madison, Madison, Wisconsin 53706, USA

Received 25 August 1980
Revised manuscript received 8 January 1981

The dipolar correlation function for a system of counterions diffusing on the surface of a polyelectrolyte cylinder is computed. The influence of screened coulombic repulsions on the dielectric increment is determined. Dissociation and reassociation of the counterions to the cylinder is treated microscopically and the coupled bulk diffusion is solved in the presence of the Poisson-Boltzmann potential. It is found that the correlation function contains a small, fast decaying, molecular weight independent part arising from diffusion around the cylinder and a large, slowly decaying, molecular weight dependent part arising from diffusion along the cylinder axis. The dissociation–reassociation kinetics can play a large, possible dominant, role in determining the relaxation rates.

1. Introduction

In a previous publication (I) [1] the coupled dynamics of counterion diffusion in bulk and on the surface of a polyelectrolyte cylinder was analyzed in order to compute the dipolar correlation function and thereby obtain a prediction for the dielectric behavior. Motion on the cylinder surface was treated as that of independent non-interacting particles and the distribution of particles along the cylinder was evaluated in terms of the coulombic repulsions of a linear array. In addition the motion in bulk was presumed unaffected by the potential generated by charges on the polyelectrolyte and other charges in solution. These restrictions are removed in this work with the aim of making the model calculation more realistic.

In the absence of internal field effects [2], the correlation function γ may be related to the complex dielectric permittivity ϵ^* (an experimental observable) via Laplace transformation (indicated by $\sim$)

$$(-\tilde{\gamma})/(-\tilde{\gamma})_{\omega=0} = \int_0^\infty -\exp(-i\omega t)(d\gamma/dt)dt/\gamma(0) = [-i\omega\tilde{\gamma} + \gamma(0)]/\gamma(0) \approx (\epsilon^* - \epsilon_\infty)/(\epsilon_0 - \epsilon_\infty)\,, \tag{1.1}$$

where

$$\gamma = \langle \mu(t) \cdot \mu(0) \rangle\,, \tag{1.2}$$

$\mu(t)$ is the system dipole moment at time t. The average is taken over the equilibrium distribution of system configurations at time 0.

We analyze correlation in position of particles which contribute to the dipole moment of the cylinder at time zero. The basis for a separation of the correlation of the dipole moment of the cylinder with associated counterions and the dipole moment of the ions in the bulk (and the solvent with which the dielectric response in bulk is correlated in a complicated manner) has been explored previously in terms of a simple two phase model [1]. For our system of n' counterions moving in the ϕ and z directions on the surface of a cylinder (length L, radius b) the dipolar correlation function is given by

0 301–4622/81/0000–0000/S 2.50

$$\gamma = e^2 \int_0^L \cdots \int_0^L \prod_i \mathrm{d}z_i' \int_0^{2\pi} \cdots \int_0^{2\pi} \prod_i \mathrm{d}\phi_i' \left\{ \hat{z} \sum_i (z_i' - L/2) + \hat{x} \sum_i b \cos\phi_i' + \hat{y} \sum_i b \sin\phi_i' \right\}$$

$$\times P_{\mathrm{eq}}(\{z_i'\}, \{\phi_i'\})$$

$$\times \int_0^L \cdots \int_0^L \prod_i \mathrm{d}z_i \int_0^{2\pi} \cdots \int_0^{2\pi} \prod_i \mathrm{d}\phi_i \left\{ \hat{z} \sum_i (z_i - L/2) + \hat{x} \sum_i b \cos\phi_i + \hat{y} \sum_i b \sin\phi_i \right\}$$

$$\times P(\{z_i\}, \{\phi_i\}, \{z_i'\}, \{\phi_i'\}, t) \,. \tag{1.3}$$

P is the conditional probability density of finding the particles (which had positions $\{z_i'\}$ $\{\phi_i'\}$ at time 0) at the sets of positions $\{z_i\}$, $\{\phi_i\}$ at time t. The dynamics includes terms describing the dissociation (and reassociation) of particles from the cylinder to the bulk. Because of the symmetry of the problem, the motion in bulk in the z (or ϕ) and r directions are independent and their effects may be analyzed separately. The two phase interpretation is preserved (even with the bulk phase starting at the cylinder surface) via non-conservation of P, i.e. P decreases with time through terms which are of the form of a probability of dissociation times one minus the reassociation probability. Particles which are not reassociated are taken to have relaxed completely whereas reassociated particles retain their correlation (except to the extent they have diffused in the z and ϕ directions). In the previous work the number of particles on the cylinder at time 0 was given by the condensation model [3]. This corresponds roughly to the most probable number derived from a grand canonical ensemble treatment (for restricted conditions of salt concentration and polyion charge density). One could compute γ for various n' (some calculations are shown in [1]) and average over n'. If the fluctuations in n' are small as they may be expected to be (for n' of DNA), the result will not change much since γ is a fairly weak function of n'. Of course n' need not be estimated via the condensation model but may be found from numerical solution of the Poisson-Boltzmann equation which appears to be useful up to conditions of moderate salt (0.1 N). This requires specification of a boundary layer inside which the n' counterions are found (at equilibrium).

2. Theory

To find γ we need to specify P_{eq} and solve the system dynamics for P. In the previous work we considered the linear case only, replaced Δr by Δz, and used a bare Coulomb repulsive potential. Replacing Δr by Δz overemphasizes greatly the short range repulsions and makes all repulsions larger than they actually are (in particular long range interactions persist). Here these approximations are relieved via use of the potential

$$V = \sum_{j<i} \sum_i e^2 \exp(-\kappa |r_i - r_j|)/4\pi\epsilon\epsilon_0 |r_i - r_j| \,, \tag{2.1}$$

κ is the Debye-Hückel screening parameter. The equilibrium distribution function is given by

$$P_{\mathrm{eq}} = \exp(-V/k_{\mathrm{B}}T) \Big/ \int_0^L \cdots \int_0^L \prod_i \mathrm{d}z_i' \int_0^{2\pi} \cdots \int_0^{2\pi} \prod_i \phi_i' \exp(-V/k_{\mathrm{B}}T) \,. \tag{2.2}$$

P satisfies the differential equation (surface diffusion with dissociation)

$$\frac{\partial P}{\partial t} = D_1\left\{\sum_i \frac{\partial^2 P}{\partial z_i^2} + \frac{1}{b^2}\sum_i \frac{\partial^2 P}{\partial \phi_i^2}\right\} - \lambda P + \lambda \int_0^L \cdots \int_0^L \prod_i \mathrm{d}z_i'' \int_0^{2\pi} \cdots \int_0^{2\pi} \prod_i \mathrm{d}\phi_i''$$

$$\times \int_0^{t'} \mathrm{d}t' F(\{z_i\}, \{\phi_i\}, \{z_i''\}, \{\phi_i''\}, t - t')P(\{z_i''\}, \{\phi_i''\}, \{z_i'\}, \{\phi_i'\}, t') . \tag{2.3}$$

Employing boundary conditions which prevent flow of ions off the ends of the cylinder and evaluating F by considering the diffusion in bulk [4,1] we obtain an analytic expression for γ (the solution is shown in Appendix I).

$$\gamma = \gamma_z + \gamma_\phi , \qquad \gamma_z = \sum_{n=0}^{\infty} \frac{-4e^2L^2}{(2n+1)^2\pi^2} R_n X_n(t) , \tag{2.4), (2.5}$$

$$R_n = \frac{\int_0^1 \cdots \int_0^1 \prod_i \mathrm{d}z_i' \int_0^{2\pi} \cdots \int_0^{2\pi} \prod_i \mathrm{d}\phi_i' \sum_i (z_i' - 1/2) \sum_i \cos(2n+1)\pi z_i' \exp(-V/k_BT)}{\int_0^1 \cdots \int_0^1 \prod_i \mathrm{d}z_i' \int_0^{2\pi} \cdots \int_0^{2\pi} \prod_i \mathrm{d}\phi_i' \exp(-V/k_BT)} , \tag{2.6}$$

$$X_n(t) = A_{nz}A_{0z}^{n'-1} \exp(-2D_{Rz}t) , \qquad \gamma_\phi = e^2b^2R_\phi X(t) , \tag{2.7), (2.8}$$

$$R_\phi = \frac{\int_0^1 \cdots \int_0^1 \prod_i \mathrm{d}z_i' \int_0^{2\pi} \cdots \int_0^{2\pi} \prod_i \mathrm{d}\phi_i' \left\{\left(\sum_i \cos\phi_i'\right)^2 + \left(\sum_i \sin\phi_i'\right)^2\right\} \exp(-V/k_BT)}{\int_0^1 \cdots \int_0^1 \prod_i \mathrm{d}z_i' \int_0^{2\pi} \cdots \int_0^{2\pi} \prod_i \mathrm{d}\phi_i' \exp(-V/k_BT)} , \tag{2.9}$$

$$X(t) = A_{1\phi}A_{0\phi}^{n'-1} \exp(-2D_{R\phi}t) . \tag{2.10}$$

Prescriptions for finding the A functions are given in Appendix I.

3. Discussion

For the potential free case $V = 0, y = 0$ (yk_BT is the Poisson-Boltzmann potential), γ has been reported previously [1]. In particular $V = 0$ yields $R_n = -2n'/(2n+1)^2\pi^2$ and $R_\phi = n'$. For small n' and weak interactions these results are approached.

Independent of the interactions as embodied in V and y the integrations over $\{z_i\}$, $\{\phi_i\}$ show that relaxation in the z and ϕ directions is independent. In addition only odd m modes contribute to the correlation function γ_z while only a single term appears in γ_ϕ. For $V = 0$ and $\lambda = 0$ we showed previously (molecular diffusion suppressed)

$$\gamma = \gamma_\phi + \gamma_z = n'e^2b^2 \exp(-D_1t/b^2) + \frac{n'8e^2L^2}{\pi^4} \sum_{n=0}^{\infty} \frac{1}{(2n+1)^4} \exp[-(2n+1)^2\pi^2D_1t/L^2] \tag{3.1}$$

and the mean squared dipole for this case is obtained by setting $t = 0$. Because of the repulsive interactions con-

tained in P_{eq} the respective amplitudes will be reduced from $n'e^2b^2$ and $n'e^2L^2/12$. Note that for given P_{eq} the amplitudes of γ_ϕ and γ_z are independent of the dynamics as described by λ, k, D_1, D_3, and y since the mean squared dipole is a static property of the system. The reduction in amplitude (dielectric increment) may be seen by comparing R_n and R_ϕ to the independent particle ($V = 0$) predictions of $-2n'/(2n+1)^2\pi^2$ and n' respectively ($R_0 = -0.2026\, n', R_1 = -0.0225\, n'$). The behavior shown by the calculations shown in table 1 is reasonable. R_0 (and R_1) and R_ϕ are close to the independent particle result for small n' but fall below it as n' becomes larger and saturation (caused by the uniform distribution, which has zero squared dipole moment, being favored strongly) occurs. R_ϕ has apparently reached its maximum value at $n' \approx 60$ and R_0 is in the vicinity of its maximum (it is easy to show that $\lim_{n'\to\infty} = 0$ for R_ϕ or R_n). Note that R_1 is larger than the independent particle prediction for small n'. For our model cylinder (DNA) a reasonable number of charged sites is 300 and an independent particle site model calculation with site occupancy restricted to zero or one would show a maximum in the dielectric response for $n' = 150$. The repulsive potential used here speeds the onset of saturation. If the particles are screened, $\kappa \neq 0$, the particles will behave more independently and R_ϕ and R_n will be closer to the independent particle result. Such behavior is apparent from the data of table 1. Once the mean distance between neighboring particles becomes less than κ^{-1} the effect of screening is lost as can be seen from the mathematical structure of eq. (2.1).

Another way to see the effect of repulsive forces on the static dielectric behavior is to increase the charge on the particles while holding L, b and n' fixed. Some calculations of this type for R_0 and R_ϕ ($n' = 10$) are shown in table 2. We define $B = e^2/4\pi\epsilon\epsilon_0 k_B TL$. Both R_0 and R_ϕ tend to zero as B increases, the effect being much greater for R_0. This confirms our picture of the role of the repulsive forces on the static dielectric behavior.

The dynamic dielectric behavior may be visualized through eqs. (2.7), (2.10), (I.18) and (I.19). The individual time dependent factors in γ (the X's) are approximately products of exponentials and hence of the form $\exp(-t/\tau)$ with τ relaxation time ($1/\tau$ a relaxation rate). All relaxation rates contain the factor $2D_R$ which arises from rotational diffusion of the cylinder. Symmetry implies that the rotational diffusion tensor is diagonal but since the diffusion around the $\tilde{z}$ axis is much faster than around the $\tilde{x}$ or $\tilde{y}$ axes we have

$$D_{Rx} = D_{Ry} = D_{R\phi} \gg D_{Rz} \,. \tag{3.2}$$

All rates contain the factor $\lambda n'$ which is a contribution to relaxation due to dissociation from the cylinder. X has a factor D_1/b^2 coming from surface diffusion in the ϕ direction whereas X_n has a corresponding factor $(2n+1)^2\pi^2 D_1/L^2$ from surface diffusion in the z direction.

The last (nonexponential) terms in eqs. (I.18) and (I.19) slow the dielectric relaxation as they subtract from the relaxation rate. For large k the integral terms are precisely λA_m and they cancel the effects of dissociation. Note that k is introduced in the boundary condition (eq. (I.14)) at the cylinder surface. This limit means that the recombination rate is so large that dissociating particles return to the chain immediately. As k increases R evolves more rapidly (in fact $\lim_{k\to\infty} R = \delta(t-t')/bD_3k$). For small k the integral term disappears. The exponential factor involving D_3 inside the integrals tends to reduce their values. Physically this corresponds to a relaxation of the fraction of particles which ultimately reassociate by diffusion in the z or ϕ directions in the bulk phase. $R(t)$ is the radial portion of the bulk particle density evaluated at the cylinder surface. Its value depends on κ as well as k. $R(t)$ was evaluated for $y = 0$ (free diffusion in bulk) and for diffusion in the Poisson-Boltzmann potential ($\kappa = \frac{1}{18} \times 10^{10}$ m^{-1} or $\frac{1}{180} \times 10^{10}$ m^{-1}) for $k = 0, 10^6, 10^9$ and 10^{13} m^{-1}. Details are given in Appendix I. Fig. 1 shows some representative results. Over the time scale for which $R(t)$ affects the dielectric response $R(t)$ is hardly affected by the Poisson-Boltzmann potential (this is not true for the "long time" behavior, $t > 10^{-10}$ s). Physically this means that a particle initially on the cylinder surface needs to diffuse only a short distance in the radial direction to be lost to the bulk phase. Over this distance (order 10^{-10} m) the potential does not change appreciably. The value of k plays a large role. Up to $k = 10^9$ m^{-1} $R(t)$ decreases only slightly as k increases. For the next few decades R decreases strongly and at $k = 10^{13}$ R has reached the point that the recombination integral term effectively cancels the dissociation term ($-\lambda A_m$).

Forcing terms in eq. (2.3) arising from the potential of eq. (2.1) are absent. Their inclusion would presumably have a detectable (possibly major) influence on the evolution of P. Incorporation of the forcing terms would force

Table 1
Integrals over the equilibrium distribution

n'	$R_0(\kappa = 0)$	$R_0(\kappa = 1/180)$	$R_0(\kappa = 1/18)$	$R_0\left(\begin{matrix}V=0\\ \kappa=\infty\end{matrix}\right)$	$R_1(\kappa = 0)$	$R_1(\kappa = 1/180)$	$R_1(\kappa = 1/18)$	$R_1\left(\begin{matrix}V=0\\ \kappa=\infty\end{matrix}\right)$	$R_\phi(\kappa = 0)$	$R_\phi(\kappa = 1/180)$	$R_\phi(\kappa = 1/18)$
2	−0.387	−0.388	−0.400	−0.405	−0.049	−0.048	−0.045	−0.045	1.993	1.993	1.995
3	−0.556	−0.561	−0.593	−0.608	−0.078	−0.076	−0.067	−0.068	2.969	2.969	2.977
5	−0.852	−0.866	−0.963	−1.013	−0.141	−0.136	−0.112	−0.113	4.86	4.86	4.89
10	−1.416	−1.459	−1.809	−2.026	−0.295	−0.284	−0.218	−0.225	9.40	9.40	9.53
20	−2.11	−2.21	−3.21	−4.05	−0.54	−0.52	−0.42	−0.45	17.3	17.4	17.9
30	−2.51	−2.65	−4.26	−6.08	−0.75	−0.74	−0.67	−0.68	24.6	24.6	25.5
40	−2.87	−3.08	−5.25	−8.11	−0.84	−0.83	−0.77	−0.90	31.9	31.6	32.2
50	−3.1	−3.3	−6.1	−10.1	−0.9	−0.9	−0.9	−1.13	35	35	38
60	−3.7	−3.9	−6.6	−12.2	–	–	–	−1.35	34	36	43

Table 2
Role of the potential in forcing the uniform distribution ($\kappa = 0$)

B	$R_0(n' = 10)$	$R_\phi(n' = 10)$
1.3706×10^{-2}	−1.416	9.39
3×10^{-2}	−1.055	9.03
4×10^{-2}	−0.9134	8.88
5×10^{-2}	−0.8056	8.76
7×10^{-2}	−0.6526	8.58
10^{-1}	−0.508	8.38
2×10^{-1}	−0.293	8.08
3×10^{-1}	−0.21	7.3
5×10^{-1}	−0.15	6.3
7×10^{-1}	−0.12	–

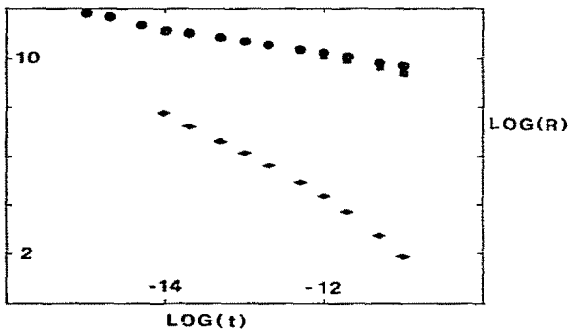

Fig. 1. Evolution of the radial density function in bulk. Circles = $k = 0$, $y = 0$; squares = $k = 10^9\ m^{-1}$, $\kappa = 10^{10}/180\ m^{-1}$; diamonds = $k = 10^{13}\ m^{-1}$, $\kappa = 10^{10}/180\ m^{-1}$.

an all numerical analysis requiring major computational effort. Investigation of this feature of the model is reserved for future work. A justification for omitting the forcing terms is given in [1] and in Appendix I.

Since our theory is for cylinders, comparison of the predicted amplitudes and relaxation times with polyelectrolyte data (especially DNA) in the literature is tenuous. Data in the literature (see [1] for references) involves (polydisperse) polyelectrolyte molecules whose lengths exceed the persistence length and whose conformations are consequently coils or wormlike chains. In addition the literature data exhibit strong concentration dependences which are unexplained. The role of the internal field must also be addressed [12]. The most comprehensive experimental study to date is that of Mandel [13]. His data on DNA exhibit a ratio of approximately two for the amplitudes of the low to high frequency dispersion regions and a ratio of about twenty for the (average) relaxation times. Our model provides upper bounds of about 10^2 for these ratios for Mandel's sample ($\lambda = 0$, no interparticle forces, cylindrical geometry). The interparticle repulsions (especially) and coiling of the molecules will reduce the ratio of amplitudes (upper bound $L^2/12b^2$) while the λ term moderates the difference between the relaxation times. There is also the possibility that induced moments track the low frequency process and reduce its amplitude.

The incorporation of the screening of the bound counterions in the calculation of the static dielectric increment amounts to involving the ions in the bulk phase in evaluating interactions between bound counterions. A consistent treatment in which the ions in the two phases do not interact (except via transport) would require the use of the bare Coulomb potential. Clearly the two phase picture imposes some unphysical constraints on the calculation.

The counterion transport takes place in a Poisson-Boltzmann potential generated from the uniform counterion distribution. A better picture would employ the potential generated from the instantaneous (evolving) positions of the bound counterions.

There remains the question of the role of the potential in affecting the surface motion of the bound counterions. For the linear case [1] we proposed that large fluctuations would not contribute appreciably to γ (through averaging using P_{eq}) and the required derivatives of the potential (when forcing terms are included in eq. (2.3)) could be obtained from the values computed from a Taylor's series expansion about the uniform distribution. Such a picture may be imposed here with the effect that a constant is added to each relaxation rate. We are currently investigating the limits of the model parameter values for which this procedure is acceptable.

Appendix I. Numerical details

As we did before [1] the forcing terms (arising from ion–ion repulsions) are omitted in the differential equation (2.3). As argued in [1] this procedure leads to dynamics which are seriously in error only for collections $\{z_i'\}$ $\{\phi_i'\}$ which differ markedly from the uniform distribution. However, these configurations have high energy (especially for many particle systems), carry little weight in P_{eq}, and hence do not affect γ. The benefit of this procedure is that we have independent particle dynamics, i.e. $P = \Pi_i P_i$ where $P_i = P_i(z_i, \phi_i, z_i', \phi_i', t)$.

To close the system of equations we require the function F which is the flux density to the cylinder at positions $\{z_i\}$, $\{\phi_i\}$ and time $t - t'$ arising from particles which left the cylinder at $\{z_i''\}$ $\{\phi_i''\}$ at time t' [4]. F is found by considering the diffusion in bulk which we treat here as forced diffusion in the Poisson-Boltzmann potential about the cylinder (previously free diffusion in bulk was assumed). For long enough cylinders the Poisson-Boltzmann potential depends only on r with the consequence that $P_i = P_{iz}(z_i, z_i' t) P_{i\phi}(\phi_i, \phi_i', t)$ and our equations separate to

$$\frac{\partial P_{iz}}{\mathrm{d}t} = D_1 \frac{\partial^2 P_{iz}}{\mathrm{d}z_i^2} - \lambda P_{iz} + \lambda \int_0^t \mathrm{d}t' \int_0^L \mathrm{d}z_i'' F_{iz}(z_i, z_i'', t - t') P_{iz}(z_i'', z_i', t') , \tag{I.1}$$

$$\frac{\partial P_{i\phi}}{\partial t} = \frac{D_1}{b^2} \frac{\partial^2 P_{i\phi}}{\partial \phi_i^2} - \lambda P_{i\phi} + \lambda \int_0^t \mathrm{d}t' \int_0^{2\pi} \mathrm{d}\phi_i'' F_{i\phi}(\phi_i, \phi_i'', t - t') P_{i\phi}(\phi_i'', \phi_i', t') . \tag{I.2}$$

Since the Poisson-Boltzmann equation employs mean fields, the diffusion in bulk is the same for all particles and the single particle (bulk) probability density c obeys (note that $c = Z(z)\Phi(\phi)R(r)$)

$$\frac{1}{D_3}\frac{\partial c}{\partial t} = \frac{\partial^2 c}{\partial z^2} + \frac{1}{b^2}\frac{\partial^2 c}{\partial \phi^2} + \frac{\partial^2 c}{\partial r^2} + \frac{1}{r}\frac{\partial c}{\partial r} + \frac{1}{k_B T}\left\{\frac{\partial c}{\partial r}\frac{\partial V}{\partial r} + \frac{c}{r}\frac{\partial}{\partial r}\left(r\frac{\partial V}{\partial r}\right)\right\} . \tag{I.3}$$

We impose the boundary conditions [4]

$$\partial c/\partial r = kc\ ,\ r = b\ ;\ \partial c/\partial z = 0,\ \ z = 0, L\ ;\ \ c(\phi) = c(\phi + 2\pi)\ ;\ \ c(z, \phi, r, 0) = \delta(z - z'')\,\delta(\phi - \phi'')\,\delta(r - b)/b\ . \tag{I.4}$$

The F functions are given by (note that they are conditional flux densities) [4]

$$F_{iz} = bkD_3\, Z(z_i, z_i'', t)\, R(b, t)\ , \qquad F_{i\phi} = bkD_3\, \Phi(\phi_i, \phi_i'', t)\, R(b, t)\ . \tag{I.5}$$

The functions Z and Φ are well known and easily found [5,1]

$$Z = \frac{1}{L} + \sum_{m=1}^{\infty}\frac{2}{L}\cos(m\pi z_i/L)\cos(m\pi z_i''/L)\exp(-m^2\pi^2 D_3 t/L^2) \tag{I.6}$$

$$\Phi = \frac{1}{2\pi} + \sum_{m=1}^{\infty}\left(\frac{\sin m\phi_i \sin m\phi_i''}{\pi} + \frac{\cos m\phi_i \cos m\phi_i''}{\pi}\right)\exp(-m^2\pi^2 D_3 t/r^2)\ . \tag{I.7}$$

Note that Φ depends on r, we have $r = b$.

The equation for R is

$$\frac{1}{D_3}\frac{\partial R}{\partial t} = \frac{\partial^2 R}{\partial r^2} + \frac{1}{r}\frac{\partial R}{\partial r} + \frac{1}{k_B T}\left\{\frac{\partial R}{\partial r}\frac{\partial V}{\partial r} + \frac{R}{r}\frac{\partial}{\partial r}\left(r\frac{\partial V}{\partial r}\right)\right\} . \tag{I.8}$$

The Poisson-Boltzmann potential V for use in eq. (I.8) is found by solving the equation [6]

$$\frac{1}{x}\frac{\mathrm{d}}{\mathrm{d}x}\left(x\frac{\mathrm{d}y}{\mathrm{d}x}\right) = \sinh y\ , \tag{I.9}$$

where $y = V/k_B T$ and $x = \kappa r$ and the boundary conditions are

$x\ \mathrm{d}y/\mathrm{d}x = 0$ at the outer boundary and

$$x\ \mathrm{d}y/\mathrm{d}x = -2Qe^2/4\pi\epsilon_0\epsilon k_B T \qquad \text{at } x = \kappa b\ . \tag{I.10}$$

Q equals the number of (permanent) charges per unit length on the polyion. The conventional method of integrating eq. (I.9) is to take a position far enough from the origin so that the linearized form of the Poisson-Boltzmann equation is sufficiently accurate. The solution of the linear Poisson-Boltzmann equation in cylindrical coordinates is well known (Debye-Hückel approximation) and the slope is just

$$\mathrm{d}y/\mathrm{d}x = -yK_1(x)/K_0(x)\ , \tag{I.11}$$

where K_1 and K_0 are modified Bessel functions of the second kind which are conveniently available as polynomials [7]. We set y to some small value (0.001 say), pick x, compute $\mathrm{d}y/\mathrm{d}x$ using eq. (I.11) and integrate numerically (fourth order Runga Kutta, the second order Poisson-Boltzmann equation yields two coupled first order equations) to $x = \kappa b$. Various choices of x are tried until the proper slope (eq. (I.10)) is found at the boundary. At this point we have a point $(y, \mathrm{d}y/\mathrm{d}x, x)$ on the full Poisson-Boltzmann potential curve and we may evaluate V and its derivatives at any r. Numerical integration of the Poisson-Boltzmann equation is hardly new and we verified our procedure by calculating some elements of Stitger's tables [6]. What is encouraging is the recent work by Fixman [8] which suggests that the potential from eq. (I.9) will be sufficiently accurate for use in eq. (I.8) for the conditions

of salt concentration and polyion charge density to which the model calculation will be applied. Numerical methods are required to solve eq. (I.8) so we postpone the succession of solving eqs. (I.9), (I.8), (2.5), (2.4), (1.3) in order to find γ.

Since the numerical methods only involve r and t the integrations over z_i and ϕ_i may be carried out analytically and the integrations over z_i' and ϕ_i' are separable (but require numerical integration). Thus γ can be constructed in pieces which facilitates interpretation of the result and comparison with our previous model calculation. By inspection of eqs. (2.4), (I.5) and (I.6) it is clear that P_{iz} may be written as

$$P_{iz}(z_i, z_i', t) = \sum_{m=0}^{\infty} Z_m(t) \cos(m\pi z_i/L) \cos(m\pi z_i'/L) . \tag{I.12}$$

Similarly

$$P_{i\phi}(\phi_i, \phi_i', t) = \sum_{m=0}^{\infty} \{\Phi_{ms}(t) \sin m\phi_i \sin m\phi_i' + \Phi_{mc}(t) \cos m\phi_i \cos m\phi_i'\} . \tag{I.13}$$

Eqs. (2.15) and (2.16) may be inserted into eq. (1.3) and the integrations over $\{z_i\}$, $\{\phi_i\}$ and $\{z_i'\}$, $\{\phi_i'\}$ performed. The former may be done analytically and we have

$$\int_0^L \cdots \int_0^L \prod_i dz_i (z_i - L/2) \cos(m\pi z_i/L) = L^{n'-1} [-2L^2/(2n+1)^2\pi^2] \tag{I.14}$$

with $m = 2n + 1$, $n = 0, 1 \ldots$; and

$$\int_0^{2\pi} \cdots \int_0^{2\pi} \prod_i d\phi_i \cos^2\phi_i = (2\pi)^{n'-1}\pi \tag{I.15}$$

with the same result for $\sin^2\phi_i$. (Note that γ separates into $\gamma = \gamma_z + \gamma_\phi$.) The integrations over the primed coordinates is more difficult and must be done numerically. The required expressions are (note change of variables) eqs. (2.6) and (2.9). These integrals were evaluated by Monte Carlo methods (successive random sampling of the configuration space) on a Harris/7 computer. Surprisingly this procedure proved more efficient than alternative Monte Carlo algorithms [9]. The potential is given by eq. (2.1). Clearly (note that z_i' goes from 0 to 1 in eqs. (2.6) and (2.9))

$$|r_i - r_j| = L\{(z_i' - z_j')^2 + (2b^2/L^2)(1 - \cos(\phi_i' - \phi_j'))\}^{1/2} \tag{I.16}$$

these results may be combined to yield $\gamma = \gamma_z + \gamma_\phi$ where

$$\gamma_z = \sum_{n=0}^{\infty} \frac{-4e^2L^2}{(2n+1)^2\pi^2} R_n X_n(t) , \qquad \gamma_\phi = e^2b^2R_\phi X(t) . \tag{I.17}$$

The solution is complete once the functions $X_n(t)$ and $X(t)$ are found. These are shown as eqs. (2.7) and (2.10). The A functions are solutions to the differential equations ($A(0) = 1$)

$$\frac{dA_{m\phi}}{dt} = \frac{-m^2D_1}{b^2} A_{m\phi} - \lambda A_{m\phi} + \lambda b D_3 k \int_0^t dt' R(t - t') A_{m\phi}(t') \exp[-m^2D_3(t - t')/b^2] \tag{I.18}$$

$$\frac{dA_{mz}}{dt} = \frac{-m^2\pi^2D_1}{L^2} - \lambda A_{mz} + \lambda b D_3 k \int_0^t dt' R(t - t') A_{mz}(t') \exp[-m^2\pi^2D_3(t - t')/L^2] . \tag{I.19}$$

Since R is found numerically the A's are given numerically also. Note that the X's are multiplied by $\exp(-2D_R t)$ (D_R is a diagonal element of the rotation diffusion tensor of the cylinder). This accounts for the effect of molecular rotational diffusion on the dielectric properties [10].

To find R a concentric cylindrical outer boundary with reflecting boundary condition ($\partial R/\partial r = 0$) is constructed. The location of the boundary is adjusted (outward) until it has no effect on the numerical results (parts in 10^4). Given κ eq. (I.9) is solved as described above to give $y(x)$ for use in eq. (I.8) (the independent variable is changed from r to x). Eq. (I.8) is replaced by a series of difference equations of variable number N (up to 1601) and the set of difference equations solved subject to the boundary conditions $\partial R/\partial r = kR$ and $R(0, b) = \delta(r - b)/b$ (the second boundary condition is satisfied only in the limit $1/N \to 0$). Finally the limit $1/N \to 0$ of $R(t, b)$ is evaluated. All this proceeded smoothly and the numerical solution for $y = 0$ agreed with the analytical solution given by Carslaw and Jaeger [5]. Since the difference equations do not satisfy a condition of the master equation [11] that the column elements of the kinetic matrix sum to zero, probability is not conserved and renormalization is required using the results from the $k = 0$ runs.

Acknowledgement

This work was supported by a National Institutes of Health Grant GM-0425.

References

[1] P.I. Meyer and W.E. Vaughan, Biophys. Chem. 12 (1980) 329.
[2] W.E. Vaughan, Ann. Rev. Phys. Chem. 30 (1979) 103.
[3] G.S. Manning, J. Chem. Phys. 51 (1969) 924.
[4] O.G. Berg and C. Blomberg, Biophys. Chem. 4 (1976) 367.
[5] H.S. Carslaw and J.C. Jaeger, Conduction of heat in solids, 2nd. ed. (Oxford University Press, London, 1966).
[6] D. Stigter, J. Colloid Interf. Sci. 53 (1975) 296.
[7] M. Abramowitz and I.A. Stegun, Handbook of mathematical functions (Dover, New York, 1972).
[8] M. Fixman, J. Chem. Phys. 70 (1979) 4995.
[9] N. Metropolis, A.W. Rosenbluth, M.N. Rosenbluth, A.H. Teller and E. Teller, J. Chem. Phys. 21 (1953) 1087.
[10] W.E. Vaughan, Adv. Mol. Relax. Inter. Proc. 12 (1978) 13.
[11] I. Oppenheim, K.E. Shuler and G.H. Weiss, Stochastic processes in chemical physics: the master equation (MIT Press, Cambridge, 1977).
[12] J.S. Anderson and W.E. Vaughan, Ann. Rep. Conf. Elec. Insul. Diel. Phen. 1976 (1978) 517.
[13] Th. Vreugdenhil, F. van der Touw and M. Mandel, Biophys. Chem. 10 (1979) 67.